



# Third-Generation Photovoltaics: Organic Photovoltaics (OPV)

Abdul Hai Alami<sup>✉</sup>, Shamma Alasad<sup>✉</sup>, Haya Aljaghoub<sup>✉</sup>,  
Mohamad Ayoub<sup>✉</sup>, Adnan Alashkar<sup>✉</sup>, Ayman Mdallal<sup>✉</sup>,  
and Ranem Hasan<sup>✉</sup>

## Abstract

The investment in novel PV technology is an important tool to exploit novel materials and material processing and manufacturing technologies to achieve performance levels that supersede those attained by classical materials and processes. The following chapter highlights the novelty of materials and processes used to produce the third-generation technology of organic solar cells and latest manufacturing technologies.

## 1 History and Background

Organic photovoltaics (OPV) are a type of third-generation solar cells that have paved the way for solution state deposition techniques that have since increased the chance of these technologies to break into their commercialization stage. Mass production of OPV from solution-based precursors will help in driving their cost down on, but on behalf of their efficiencies. However, utilizing these technologies in multi-junction devices that are based on the difference in bandgap of different junctions can drastically increase their

respective efficiencies with a slight increase in cost. A global aim is set by researchers to accommodate to both high throughput production of PV, specifically OPV, and similar third-generation technologies using roll-to-roll compatible techniques while retaining relatively good efficiencies in comparison with the devices that are produced in research and development centers, with utilizing solution processing methods at low temperatures and eliminating the use of expensive vacuum techniques.

The term organic refers to the existence of hydrocarbon molecules, with less than a 10,000 molecular weight, or chains (polymers), with more than 10,000 molecular weights of hydrocarbons inside a specific compound. The discovery of the organic semi-conducting material is accredited to John McGinness through his utilization of it in the “melanin (polyacetylenes) bistable switch”. Along the organic semi-conducting material timeline, anthracene which is a solid polycyclic aromatic polymer (three fused benzene rings), was used as the first organic light-emitting device. Moreover, a breakthrough in the 1980s occurred when Kodak reported the first organic light emitting and solar cell device (A brief history of OLEDs).

There are different aspects to tackle in OPV, just as mentioned earlier going from lab to commercial scale production is going to be a crucial turning point in this technology's future, selecting the appropriate tools and processes can be thought of as the initial step into achieving this sought-after goal. However, characterization and testing techniques such as a certified STC sun simulator to ensure the integrity of the produced cells, UV-Vis tests, scanning electron microscope tests, cyclic voltammetry, etc., must be utilized in the optimization process before the mass production of these technologies in order to provide a consumable-worthy product. OPV are a work in progress, with a current champion efficiency of 18.2% according to the national renewable energy laboratory (NREL) (Organic Photovoltaic Solar Cells). OPV are based on organic active layers sandwiched between two electrodes. Light passes

A. H. Alami (✉) · H. Aljaghoub · M. Ayoub · A. Mdallal ·  
R. Hasan

University of Sharjah, Sharjah, United Arab Emirates  
e-mail: aalalami@sharjah.ac.ae

H. Aljaghoub  
e-mail: haljaghoub@sharjah.ac.ae

M. Ayoub  
e-mail: mohamad.ayoub@sharjah.ac.ae

A. Mdallal  
e-mail: ayman.mdallal@sharjah.ac.ae

S. Alasad · A. Alashkar  
American University of Sharjah, Sharjah, United Arab Emirates  
e-mail: g00070854@aus.edu

A. Alashkar  
e-mail: b00028197@alumni.aus.edu

through a transparent substrate which could be a transparent conductive oxide (TCO)-coated glass or a flexible substrate; however, it is favorable to use a flexible material since it can be processed at low temperatures which reduces the overall power consumption. On flexible substrates, indium tin oxide (ITO) is deposited, usually via sputtering, which allows holes to be collected. This part allows the light to pass, and any electrons generated will be conducted through the ITO. PEDOT:PSS is one of the most important materials utilized for the motion of holes, as it is a hole transport material (HTM) and once the light hits it, holes are allowed to pass while electrons are blocked. The active material is an organic donor/acceptor blend, as will be discussed later. A photon comes with a certain amount of energy  $h\nu$ , hits the surface of the active material inside an organic solar cell (OSC), where an electron and a hole are generated. The donor donates electrons, leaving holes behind, and the acceptor accepts the electrons that would fill the intrinsic concentration of the holes available. Aluminum is usually used as a cathode for electrons collection from the device, silver, or calcium.

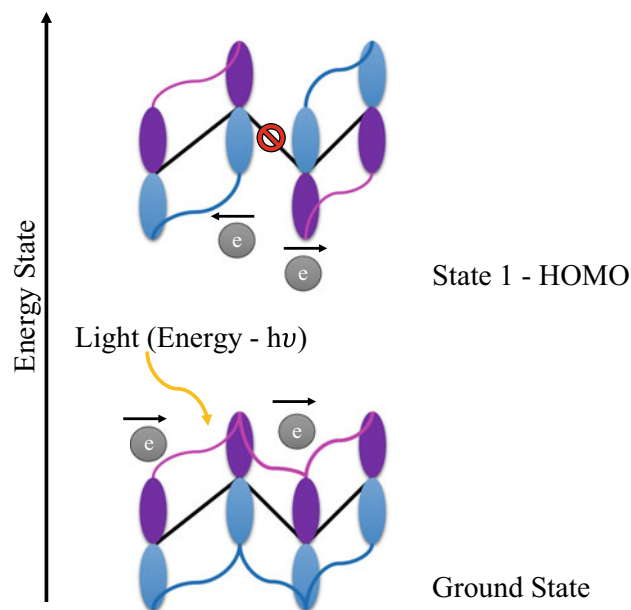


**Fig. 2** Energy states and  $\pi^*$  orbitals' shift with added energy—ground and state 1

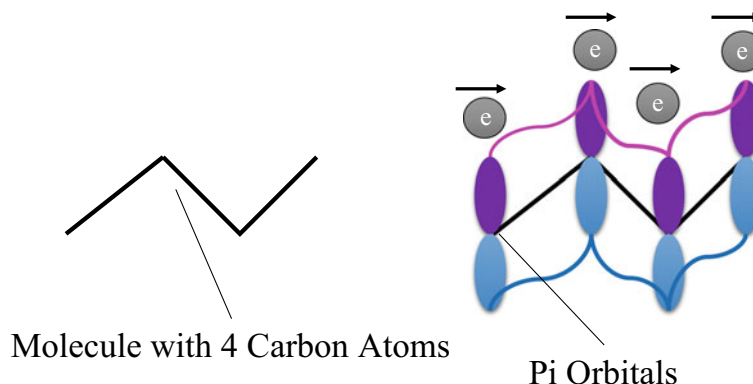
## 2 Physics of Organic Photovoltaics

In a conjugated organic system, each carbon atom corresponds to a  $\pi^*$  orbital that allows electrons to hop across the molecule. For a system with  $n$  carbon atoms, at the lowest energy state, there are  $n$   $\pi^*$  orbitals that are perfectly aligned and allow electrons to meander throughout the organic molecule, such as shown in Fig. 1. When energy is added to the organic molecule, via light absorption for instance, corresponding nodes pop up in between the  $\pi^*$  orbitals creating an unsymmetrical path for electrons (an anti-parallel formation), such as shown in Fig. 2. Given that out of these two states (the occupied energy levels), state 1 has a higher energy level, and in the case of light absorption, electrons are most likely to be divided between these two states,

making state 1 the highest occupied molecular orbit (in terms of energy), also known as the HOMO level.

Adding further energy to an organic molecule will split the  $\pi^*$  orbitals even further, creating a parallel formation with only one couple of  $\pi^*$  orbitals, singling out the other two. This will further block the motion of electrons by creating an extra node in the organic molecule. By going further and adding extra energy, more nodes are created between the  $\pi^*$  orbitals until all the orbitals are singled out and electrons are exclusive to their home orbital such as shown in Fig. 3. Out of the top two energy states (the unoccupied energy levels), state two has the lowest energy level, making it the lowest unoccupied molecular orbit when there is excess energy within the organic molecule system, also known as the LUMO level.

**Fig. 1** Ground state molecule with aligned  $\pi^*$  orbitals



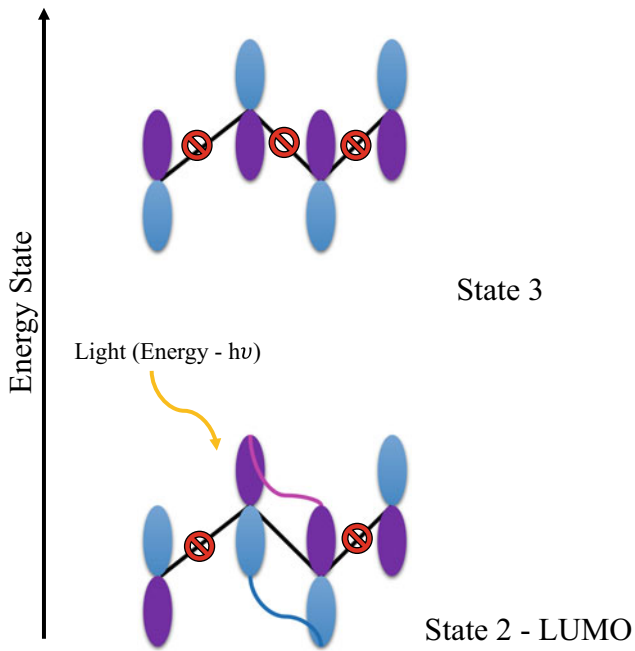


**Fig. 3** Energy states and  $\pi^*$  orbitals' shift with added energy—state 2 and state 3

The difference between the HOMO and LUMO levels of an organic molecule is equivalent to the bandgap in non-organic materials, which is the energy barrier required to free an electron from the ground state to a state that can allow the collection of electrons in the form of electric

current, shown in Fig. 4. Since both the HOMO and LUMO levels are so close in energy, and with the vacancies available in the LUMO level, electrons are easily excited and transition smoothly between these states, with the gain and loss of energy.

### 3 Organic PV Cell Structure

The highlight of third-generation solar cells in general, and specifically OSC in this case, is the deviation from the conventional P–N junction that is utilized in first generation crystalline silicon and second generation thin-film technologies. With conventional P–N junction structures, the diffusion length of minority carriers, electrons in P regions and holes in N regions, is very short, leading to recombination events that ultimately decrease the amount of electrical current and power extracted from a given cell. However, in third-generation solar cells, this issue has been widely studied and alternatives were implemented. Throughout the development OPV, three structures have played major roles in allowing this technology to reach the condition it is in today. The single layer organic solar cell (OSC) consists of a substrate (usually ITO- or FTO-coated glass), a semi-conducting polymer and a metal contact, such as shown in Fig. 5. In this structure, a relatively weak electric field is produced between the metal contact and the transparent conducting oxide (TCO), and the semi-conducting organic material (the polymer) is used as an

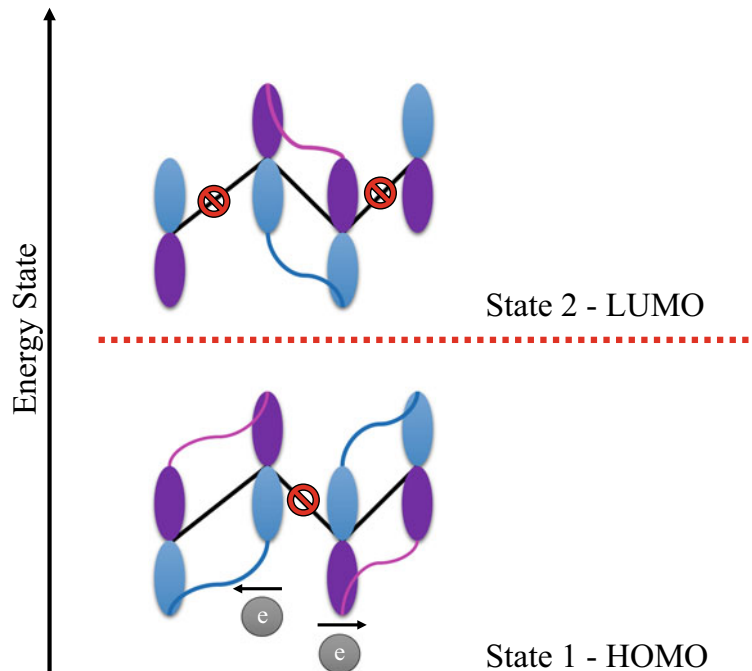


**Fig. 4** HOMO and LUMO levels

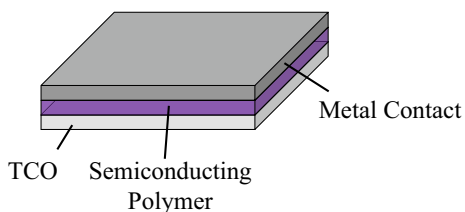


**Fig. 5** Single layer OSC structure

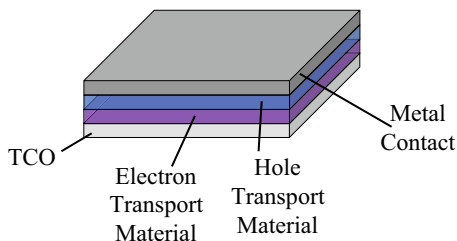


**Fig. 6** Bilayer OSC structure

electron and a hole diffusion layer. This structure performs weakly due to the insufficient electric field intensity for charge separation, which leads to more recombination events and loss of electrons which subsequently leads to loss of efficiency.

Next in line comes the bilayer OSC, which contrary to the single layer OSC, the single layer polymer is split into electron and hole diffusing layers which provide a relatively better electric field and ensures a better separation process, such as shown in Fig. 6. The short diffusion length of minority carriers (electrons in the hole diffusing layer or holes in the electron diffusing layer) acts as an adversity that accompanies this scheme of device design. In addition to these layers exists the metal contact and the TCO for charge collection.

Currently, the dominant structure in research for OSC is the bulk-heterojunction (BHJ). It was first investigated by Heeger and Friend (Yu et al. 2014), where they reported the use of a mixture consisting of solid state donor and acceptor that provides a nanostructured morphology. In BHJ-OSC, the short diffusion length of minority carriers is overcome by creating an interconnected electron and hole transport materials which interact in the form of a network, such as shown in Fig. 7a, c. The generated electrons and holes are injected in their respective diffusion layers and move across the OSC at an instant, providing high separation efficiency and a better chance for these charges to be collected using the metal and the TCO at both ends of the OSC and a PEDOT-hole transporting layer into the top contact. An aligned BHJ-OSC was also introduced which ensures that island regions of sole hole or electron diffusing materials are avoided, such as shown in Fig. 7b, d.

## 4 Materials and Fabrication Techniques

Currently, research is mainly done on two materials for the BHJ active layer consisting of P3HT and PC<sub>60</sub>BM. These two materials are commercially obtained in powder form, and the precursor is prepared by dissolving these powders into solvents such as chlorobenzene (CB), that is after optimizing their ratios and the amount of solvent used. The mainstream deposition techniques for OSC in research and development is spin coating and to a lesser extent, slot-die deposition, although other techniques have been devised as well, and are compared in terms of layer thickness accuracy, amenability to roll-to-roll production and material waste. Spin coating heavily depends on the wetting of the substrate, the viscosity of the precursor used, the speed and time at which the spin coater rotates. Post-treatment is usually required and its conditions include annealing (heating the deposited layer), anti-solvent treatments, quenching, etc. This information will be discussed in detail in the dedicated manufacturing techniques chapter.

### 4.1 Solvents

An issue arises with the use of the previously mentioned solvent, CB, and di-chlorobenzene (DCB), which is also commonly used in OPV, as they present health and environmental hazards. Working with either CB or DCB limits the production of OSC to controlled environments such as that provided by a glovebox, and it also draws back the commercialization of this technology given the direction the world is headed into preserving the environment and controlling pollution levels. Although the end devices while using CB or DCB as precursor-solvents are relatively good, alternatives must be sought to counter these issues.

Poly(3-hexylthiophene-2,5-diyl), also known as P3HT, is a polymer that is extensively used in OPV applications, as well as organic light-emitting diode (OLED) and organic field-effect transistor (OFET) applications, P3HT's chemical structure is shown in Fig. 8, with the chemical formula (C<sub>4</sub>H<sub>2</sub>S)<sub>n</sub>. P3HT has a low bandgap (~1.9 eV (Murali et al. 2015)), which means that it absorbs a wide range of the ultraviolet and visible light spectrum. In a BHJ active layer blend, P3HT acts as the donor material, providing a pathway for holes to be transferred across the OPV cell. P3HT is highly soluble in the previously discussed solvents CB and DCB, and with its fast drying characteristics, it results in a highly crystalline absorption thin film (Polymer).

Fullerene derivative (Brinkmann et al. 2010; Brinkmann et al. 2010)-phenyl-C<sub>61</sub>-butyric acid methyl ester (C<sub>72</sub>H<sub>14</sub>O<sub>2</sub>), known as PCBM, is a soluble derivative of C<sub>60</sub>, that is commonly used in OPV, and has a chemical structure

**Fig. 7** **a** Bulk-hetero junction OSC, **b** Aligned bulk-hetero junction OSC, while **c** is a depiction of BHJ and **d** is that of aligned BHJ

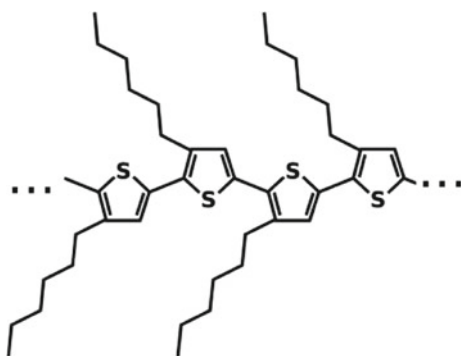
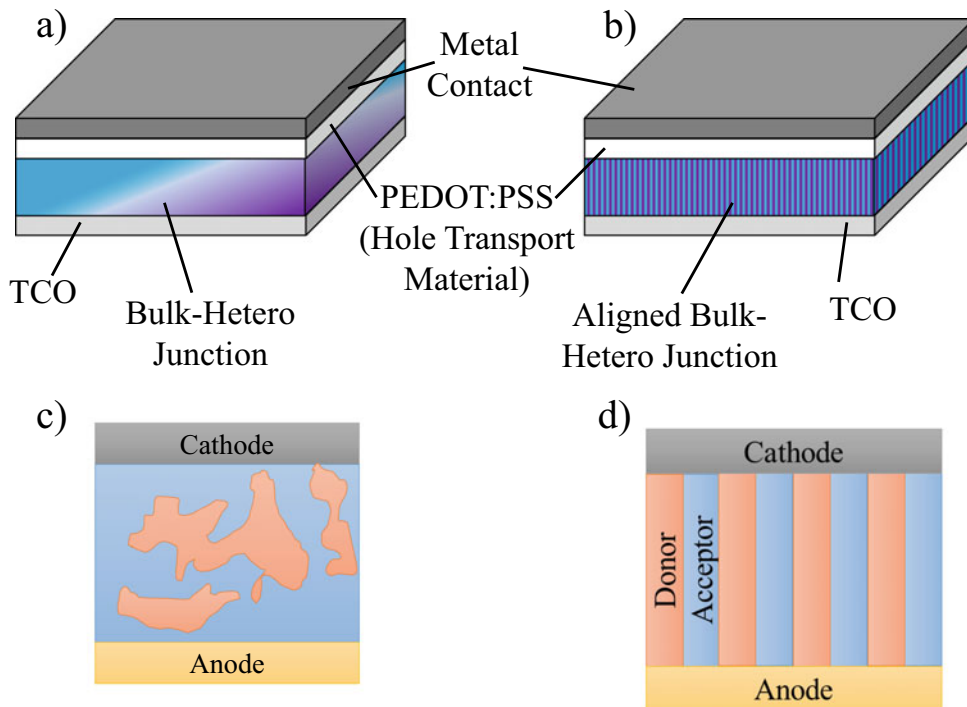


**Fig. 8** P3HT chemical structure (Brinkmann et al. 2010) (<http://gisaxs.com/index.php/Material:P3HT>)

such as shown in Fig. 9. PCBM is an electron acceptor, that is used as an electron transporting material inside BHJ structures of OSC, it has a bandgap of 2.4 eV with a high electron mobility for efficient charge transfer across an OSC. It is easily soluble in donor polymer solvents such as CB and DCB and mixes well with other materials such as P3HT to create a state-of-the-art BHJ absorption layer.

## 4.2 Hole-Transport Materials

In OSC, a hole transporting material (HTM) is usually deposited on top of the BHJ layer, in order to enhance the mobility of the holes and increase the chances of

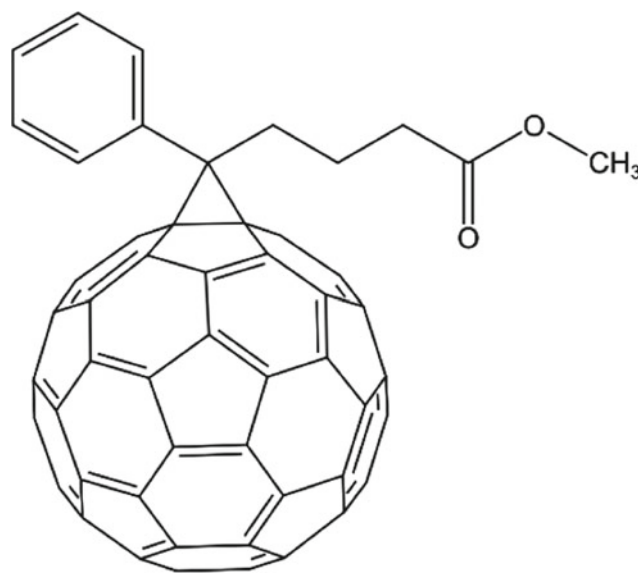


**Fig. 9** PCBM chemical structure (“Phenyl-C61-butyric acid methyl ester” 2021)

collecting them using the top electrode (Silver, gold, ITO, etc.). Poly(3,4-ethylenedioxythiophene) polystyrene sulfonate, known as PEDOT:PSS, with the structure shown in Fig. 10, is a common transparent conducting polymer that is used as an HTM. It has a high conductivity and a desirable level of transparency, along with a solution-metering capability making it a key material for OPV applications.

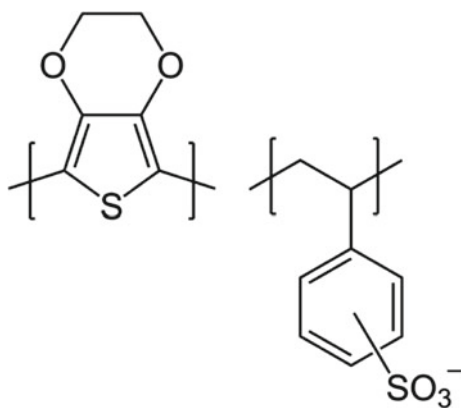


**Fig. 10** PEDOT:PSS chemical structure (Brinkmann et al. 2010) ([https://en.wikipedia.org/wiki/PEDOT:PSS#/media/File:Polythiophenes\\_Pedotpss.png](https://en.wikipedia.org/wiki/PEDOT:PSS#/media/File:Polythiophenes_Pedotpss.png))

### 4.3 Deposition on Substrates

OSC substrates have some requirements that have been standardized to ensure a high-performance of the end devices. A high-quality optical transparency is essential to allow for a high-intensity of the incident light to reach the photoactive layer with its different designs (single junction, bilayer and bulk-heterojunction), given that OSC are usually operated in a flipped position relative to the deposition sequence. In some cases, OSC are manufactured using non-transparent substrates. However, the architecture of the device can be affected by the utilization of non-transparent substrates due to the requirement of top electrodes to be transparent with a transparent top barrier (stuck to the substrate). While by using transparent substrates, the transparent electrodes often combined with it can be placed either on top or on the bottom or on both sides for semi-transparent cells. The smoothness of the substrate is also an important parameter to consider, more importantly, the rms roughness of the substrate, which controls the nucleation and crystallization rate of the subsequent layers with positive effects to the interface resistance. Thickness up to the nanometer range is fine for the case of glass or PET to enhance high-quality deposition of the subsequent layers. Roughness of the surface should not be high when the distances of structures are not long since it produces shorts in the device. When the distances are long, moderate roughness can be accepted. An example of rough substrates over short and long distances are metals, while substrates composed of plastics are only rough at long distances. Being thermally resistant is a must for OSC substrates, given that the deposited layers (ETMs, active and HTMs) are processed “annealed” at high temperatures, reaching up to 500 °C, which also corresponds to a high dimensional stability. Chemical resistance to what is considered to be lethal components that make up OSC, is

something that must be considered with the highest regard, given how effective the solvents that are used in penetrating through surfaces. Low water absorption is taken into account for the long-term operation of OSC, due to the adverse effects water molecules have on the active materials in OSC, and having a low water absorption will ultimately increase the lifetime of the fabricated devices.

#### 4.3.1 Glass Substrates

Fluorine-doped tin oxide, or indium tin oxide-coated glass is a conventional substrate that is used for OSC applications. With a 92% transmission in the visible light spectrum and 600 °C maximum processing temperature, it makes for a convenient device fabrication. The relatively lighter weight of glass substrate can be an advantage in comparison with metal substrates (stainless steel), 220 mg/m<sup>2</sup> versus 800 mg/m<sup>2</sup>, respectively. Stainless steel substrates are also a setback in terms of visible light transmission at 0%, but have a high tolerance for higher temperature processing if required. (Fthenakis 2012). The problem associated with using glass is its brittleness and ability to break while processing. However, substrates like glass can be used in many applications in the context of housings’ exterior, such as windows. Glass substrates are preferred over plastics, which will be discussed in the following section, due to their high transparency in the visible spectrum and high resistance to UV. The low light transmission of stainless steel eliminates its use as a photoanode to allow the light to pass in. However, stainless steel can be used when the operating temperature exceeds the limit of that of glass substrates (>1000 °C). Stainless steel also shows better dimensional stability than glass or plastic substrates. Metal foils can also withstand high processing temperatures and are dimensionally stable, but their use is limited since they are non-transparent and have a high surface roughness, which can be overcome to some extent using polishing techniques. However, metal foils with no transparency can be utilized when the light is incident on the cell in its top position.

#### 4.3.2 Flexible Substrates

Flexible substrates are utilized for roll-to-roll production lines to bring down the overall cost of OSC. Polyethylene terephthalate (PET) substrates are optically transparent to visible light, with an 89% transmission, and have outstanding low moisture absorption at 0.14% and high-quality mechanical properties with a 5.3 GPa (Fthenakis 2012) Young’s modulus and a 225 MPa (Fthenakis 2012) tensile strength. Polyethylene naphthalate (PEN) is a polymer with comparable properties and used in the same context of PET. However, these substrates have a low maximum processing temperature at 78 and 121 °C (Fthenakis 2012), respectively. For high-temperature processing requirements,

Polyimide (PI) is a polymer with relatively good mechanical properties, that retains a good degree of flexibility, and a novel 410 °C (Fthenakis 2012) processing temperature for high-temperature OSC materials.

#### 4.4 Compatibility with Roll-To-Roll

Operating a roll-to-roll production line is an achievable task and very beneficial on the long run for any process or fabrication that can be easily metered, which is the case for OPV, given that these lines can operate 24/7. However, there are points to be considered before optimizing such a process which are, the type of ink used, wetting and dewetting of the substrate, given that in order to make the roll-to-roll successful it is important to make sure that the material wets the surface, the thickness of the layer to prevent layers from intermixing, managing the self-assembled process, oxidation, contamination, or defects are reduced or completely avoided.

The choice of the deposition technique in a roll-to-roll line depends on the thickness of each layer, deposition events, annealing conditions, ink properties, solvents, substrates, and viscosity. The choice of the deposition technique mostly depends on the viscosity of the ink that affects its

deposition on the substrates (too low viscosity can cause evaporation or leakage as well as preventing the formation of very sharp edges, and high viscosity makes it very difficult to cover the entire surface). Viscosity of ink in the photoactive layer has to be low due to the limited solubility of the photoactive compounds. P3HT/PCBM (Poly3-hexylthiophene (P3HT) and [6,6]-phenyl-C61-butyric acid methyl ester (PCBM)) active material has a viscosity of 1–5 mP.s. But in the case of other layers such as PEDOT:PSS, it is not limited to a very low viscosity and can reach above 50 mPs. Silver inks can be synthesized with low viscosity and are ink jet printed or can be in the form pastes and subsequently screen printed.

Figure 11 shows the inkjet-printed silver grid where the height is 300 nm from (b) the line profile and (c) the screen printed TEC-PA-010 ink from Inktec (<http://www.inktec.com>) with height of 2000 nm as shown in (d) the line profile (Inktec). The conductivity of grid is higher in (c) due to increased line height. Therefore, it would be good to make sure that the topology or deposition process is going to increase the size of the lines. Figure 12 shows a comparison in the current density of the simple ITO, silver which is highly conductive in honeycomb structure with PEDOT, and silver lines with PEDOT. The I-V curves of

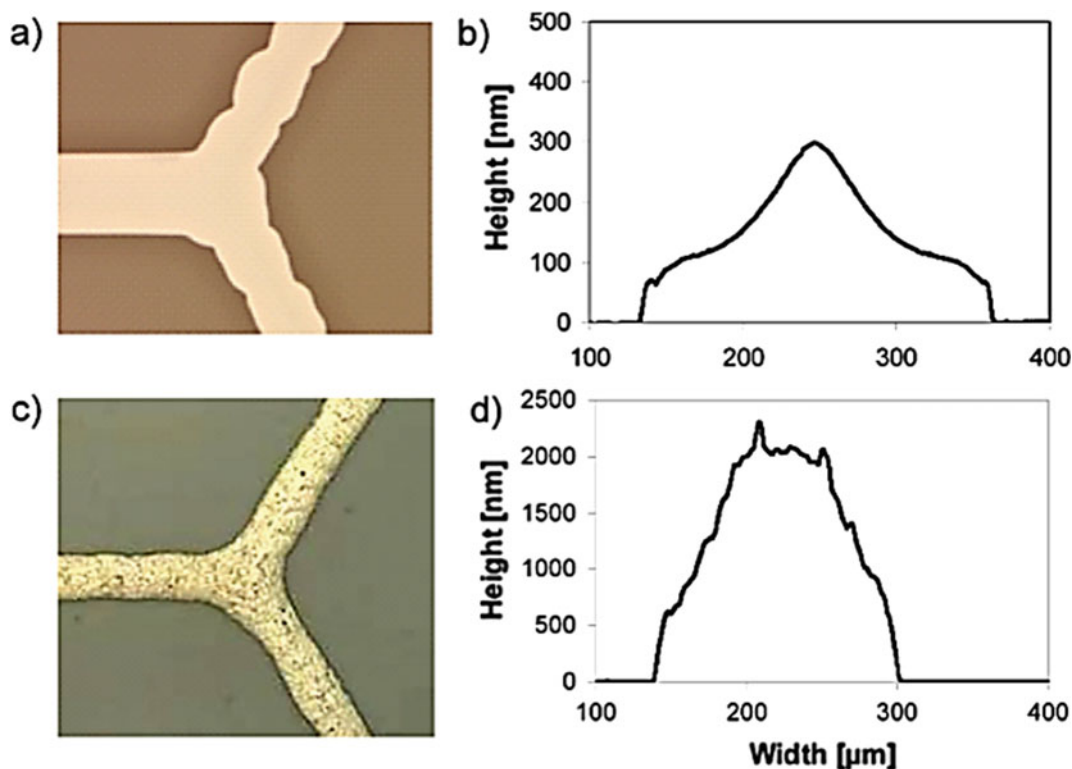


**Fig. 11** a Microscopic image of inkjet-printed silver grid on PEN substrate and b its line profile. c Microscopic image of Inktec TEC-PA-010 ink screen printed and d its line profile (Galagan and Andriese 2012)

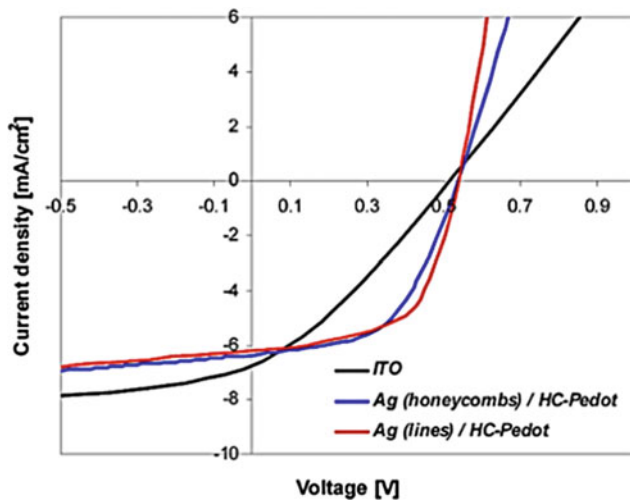


**Fig. 12** Comparison between the current density versus voltage for grids and ITO-based devices (Galagan and Andriessse 2012)

the solar cells show that there is a lucrative advantage of using such grids.

#### 4.5 Spin Coating for OPV Manufacturing

In recent days, the processing of OPV utilizes techniques of coating and printing. Developing such solar cells is mostly done by spin coating. This is one of the most important manufacturing processes used in laboratory scale cells, while other coating and printing techniques are analytic to the parameters associated to the ink and the surface interaction. Spin coating is not analytic which is a major advantage. This technique is, however, not compatible with roll-to-roll processing which involves processing of the solar cells in liquid form or in solution, to be able to deposit one layer after another on a substrate. OPV devices are mostly distinguished by roll-to-roll production lines. Although they can be handled simply and are fast to process, it is still difficult to transform all the lab-scale

processing parameters to large scale, specifically with techniques not compatible with roll-to-roll (Arbouch et al. 2014). Figure 13 shows the operation of spin coating where the solution is deposited on the top of a rotating disk. Due to centrifugal force, the material spreads on the whole surface. Only a little amount of the material is needed, after spinning, it covers the whole exposed surface and then it is heat-treated/annealed to have a homogeneous and a low-resistance layer.

Spin coating and annealing parameters can both be optimized to result in an efficient active organic layer. The optimization is carried out by testing different spin coating frequencies and durations, as well as annealing temperatures and time. Shaban et al. (2021) studied the effects of these parameters on a P3HT:PCBM active layer blend where the spin coating frequency ranged from 900 to 3000 rpm and the annealing temperature ranged 130–190 °C. Not only does the energy efficiency of an OSC get affected by these conditions and parameters, but the optical efficiency, which depends on the thickness of the end layer, is noticeably variable, such as shown in Fig. 14. Optimum performance values, based on their obtained J-V curves, correspond to 3000 rpm spin coating frequency and 160 °C annealing temperature. With increasing the annealing temperature starting from 130 °C,  $J_{sc}$ ,  $V_{OC}$  and power conversion efficiency (PCE) values increase from 8.82 mA/cm<sup>2</sup>, 0.597 V, 1.95% to a threshold of 10.78 mA/cm<sup>2</sup>, 0.640 V and 3.68% at 160 °C, and reaching a low of 8.24 mA/cm<sup>2</sup>, 0.664 V and 2.21% at 190 °C.

Using an Mg–Al cathode blend and ranging the spin coating frequency from 900 to 3000, the performance values  $J_{sc}$ ,  $V_{OC}$ , and PCE increase from 8.649 mA/cm<sup>2</sup>, 0.639 v and 2.61% to 12.01 mA/cm<sup>2</sup>, 0.660 V and 4.65%, respectively. The effects of annealing on different solvents for organic active layer blends are also worthy of being studied. Figure 15 and Table 1 show the effect of annealing on the absorbance and J-V curves for blends that utilize chlorobenzene and o-Xylene, where enhancement is found in both compositions after annealing.

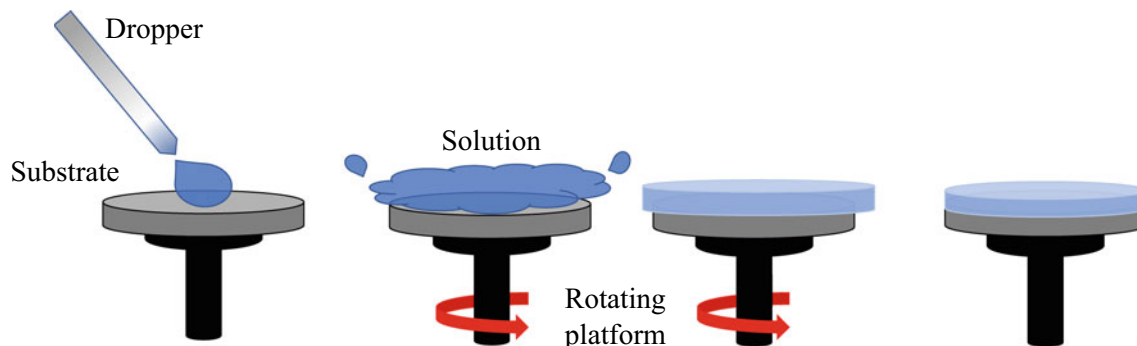


**Fig. 13** Spin coating process



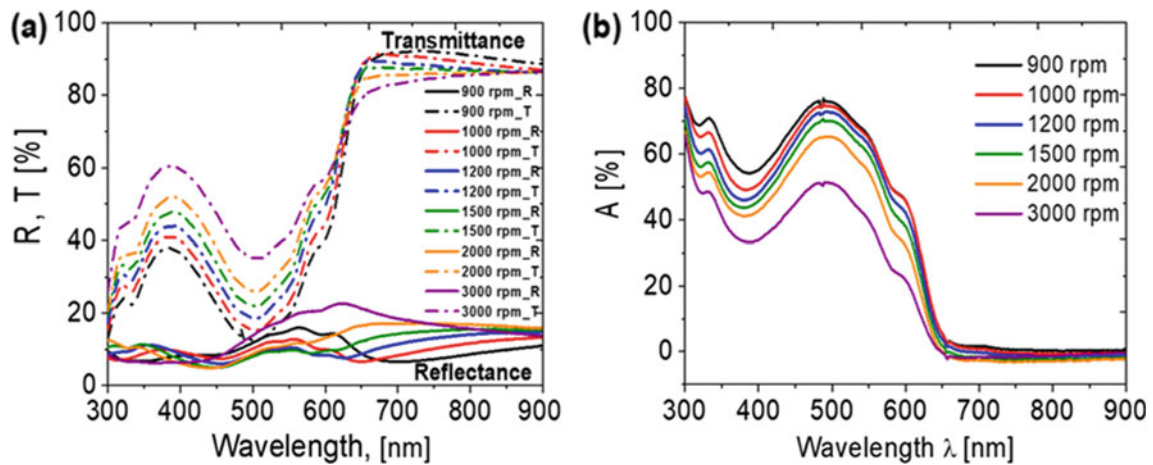


**Fig. 14** a Reflectance and transmittance b Absorbance for P3HT:PCBM blend at different spin coating frequencies and annealed at 160 °C for 5 min (Shaban et al. 2021)

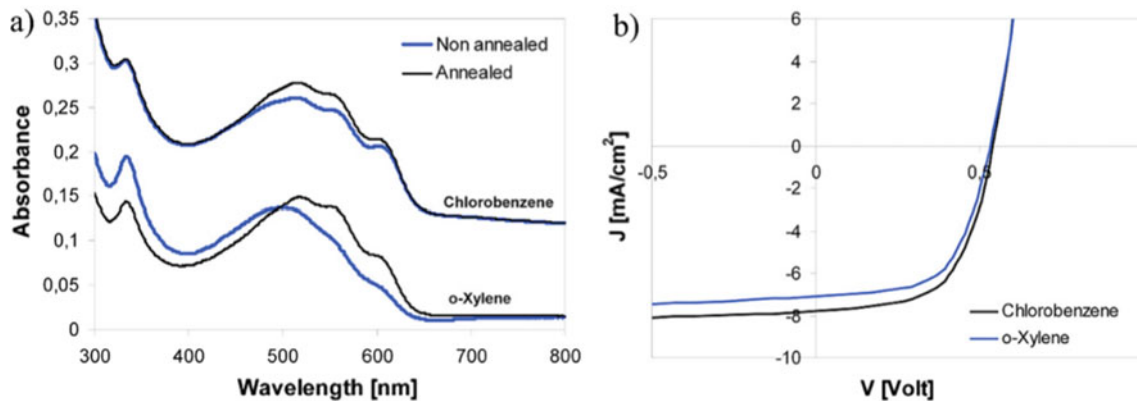


**Fig. 15** a Effect of annealing on absorbance and b J-V characteristic curves (Galagan and Andriess 2012)

**Table 1** Effects of annealing temperature on organic active blends' performances (Galagan and Andriess 2012)

| Solvent, annealing          | $J_{sc}$ (mA/cm <sup>2</sup> ) | $V_{oc}$ (Volt) | FF    | $\eta$ (%) |
|-----------------------------|--------------------------------|-----------------|-------|------------|
| Chlorobenzene, not annealed | 3.64                           | 0.572           | 0.296 | 0.62       |
| Chlorobenzene, annealed     | 7.75                           | 0.546           | 0.572 | 2.42       |
| o-Xylene, non-annealed      | 4.71                           | 0.507           | 0.332 | 0.79       |
| o-Xylene, annealed          | 7.05                           | 0.535           | 0.581 | 2.19       |

#### 4.6 Slot-Die Coating

A roll-to-roll compatible technique is slot-die coating, where a material is added using a die head that allows the material to fall down in a vertical direction through its slot, while the slot-die head is moving relative to a stationary stage. This coating technique allows for roll-to-roll coating of the hole transport layer (PEDOT:PSS) and the photoactive layer (P3HT/PCBM). Layers deposited with slot-die can have very low thickness and be uniform. 1-D patterning can be used to make the OPV modules. The deposition

profile, shown in Fig. 16, can be characterized by applying different techniques including Atomic Force Microscopy (AFM), which consists of a small needle that moves right and left on the surface. If the surface is smooth, a flat line is produced, and if there were rough particles, it will be shown from the diagram. The average thickness of the layer is about 110 nm for the PEDOT:PSS using the speed of about 10 m/min (the optimum one) and using a drier at 110 °C. The other way of measurement is using the ellipsometry where the index of refraction of the material is measured to get the thickness.

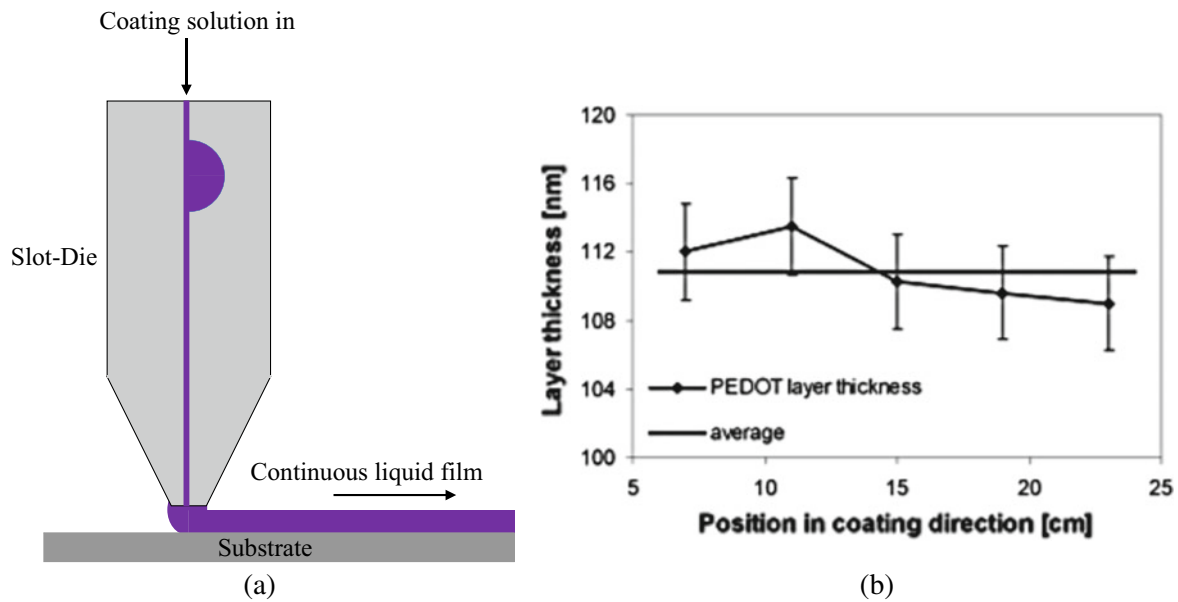


**Fig. 16** a Depiction of the slot-die deposition process and b layer thickness versus position in coating direction (Galagan and Andriesse 2012)

#### 4.7 Overall Fabrication Process

Fabricating an OSC comprises of different stages that are mostly done in controlled environments. To begin with, an FTO or ITO-coated glass is cut and cleaned in preparation for a residue-free process. Then using chemical etching, a narrow region on the coated glass substrate is removed to allow for latter top contact deposition. The layers that make up an OSC are deposited (mainly using spin coating), where it goes as follows, electron transport layer (ETM), usually Titanium Dioxide ( $\text{TiO}_2$ ), organic active blend (the BHJ), an HTM (PEDOT:PSS), and a thermally evaporated silver or gold contact, with the addition of annealing steps in between different layers' depositions for better sintering, crystallization and formation of the desired end materials.

#### 4.8 Scaling up OPV for Commercial Use

One of the things researchers are interested in is scaling up. Scaling up means going from a lab-scale product to a commercial one, with a larger active area is required. However, as a consequence, there may be a lot of losses that will arise from the larger thicknesses that the ions or the electrons/holes (charge carriers) have to pass, such as recombination. These losses mainly depend on the sheet resistance of the electrode. Testing a cell with an active area

of  $0.09 \text{ cm}^2$  can yield an efficiency of 2.42%. By scaling up and having a higher active area of  $6 \text{ cm}^2$ , the current will decrease, and voltage will decrease slightly but the fill factor will be affected significantly, and hence, the overall efficiency will show a sharp drop indicating a worse performance. In this case, an efficiency loss of around 20% is witnessed using devices based on ITO-coated glass substrates and shows the performance of devices with active areas of  $0.09 \text{ cm}^2$  and  $6 \text{ cm}^2$  as shown in Table 2.

As interconnecting solar cells provides high voltages, the coating and printing processes can be used to establish direct patterning. Patterned printing has emerged to manufacture modules with internal interconnecting. The easier way of connecting cells/modules is having a common internal connection, where a photoanode and one common back surface field are utilized. All of the components share the substrate but each of them has unique/individual active areas and modules printing may offer a significant reduction in the manufacturing cost and increase the stability of the modules.

In ITO, the cell's width is restricted between 0.5 and 1 cm as a result of the high sheet resistivity; hence, ohmic losses are decreased. However, bigger areas are essential to get more energy from solar radiation. Interconnection of individual cells serves as an alternative to accomplishing high efficiency rather than increasing the size of the cells. The performance for the two cells with  $0.09$  and  $6 \text{ cm}^2$  is shown in Fig. 17, and the efficiency for the smaller cells

**Table 2** The performance of devices with active areas of  $0.09$  and  $6 \text{ cm}^2$  (Galagan and Andriesse 2012)

| Active area ( $\text{cm}^2$ ) | $J_{sc}$ ( $\text{mA}/\text{cm}^2$ ) | $V_{oc}$ (V) | FF    | $\eta$ (%) |
|-------------------------------|--------------------------------------|--------------|-------|------------|
| 0.09                          | 7.75                                 | 0.546        | 0.572 | 2.42       |
| 6                             | 7.46                                 | 0.530        | 0.478 | 1.89       |

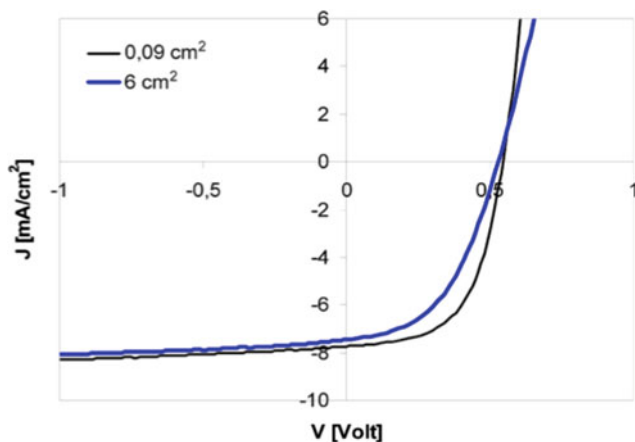


**Fig. 17** Performance of two organic cells of different areas (Galagan and Andriess 2012)

interconnected together is 20% higher than the one big cell (seen from the higher energy). By increasing the width of the cell above 1 cm, the losses in efficiency increase significantly.

#### 4.9 Recent Progress of Organic Solar Cells

Over the past 3 decades, OPV have showed decent progress due to their low cost of fabrication, easy processing techniques, with liquids metering and roll-to-roll production lines, and flexibility. The efficiency for this technology has exceeded 18.2% (Best Research-Cell Efficiency Chart) for single junction devices and 14.2% (Best Research-Cell Efficiency Chart) for multi-junction tandem device structures (Sharma et al. 2022). OPV have been implemented in a variety of applications so far. Indoor power generation is one of the main applications for OPV given the advantages that indoors have over outdoor light harvesting conditions (below 1 sun intensity), given that the light spectra of indoor sources match well with the light absorption coefficients of OPV materials, and even if there was a low match, optical properties of these materials are easily tuneable (Ryu et al. 2020). Different active layer blends have been used and ratio-optimized such as PCDTBT:PC<sub>71</sub>BM and PTB7-Th:PBDB-T:ITIC-Th:PC<sub>71</sub>BM and have shown efficiencies reaching 16% and 14%, respectively, with indoor conditions based off different light sources and spectrums (fullerene and LED). Increasing the efficiency of OPV devices have been targeted by researchers and attempted by utilizing techniques such as the singlet fission (SF). The singlet fission is a technique that is used to multiply the quantity of photons reacting with the active layer in an OSC, where a singlet excitation energy state is converted into two spin-triplet excitons. The newly multiplied photons carry less energy than the initial incident photon but given

that charge carriers' generation is independent of the energy of a photon and more dependent on the number of excitation events, more carriers are generated and subsequently an increase of current is obtained as well as an increase in efficiency (Sharma et al. 2022). Optimizing the ratio of active layer blends helps in the singlet photon fission regard as well as narrowing down the bandgap of the active material (HOMO–LUMO) energy difference to utilize a larger portion of the light spectrum and increase the excitation events overall.

#### 4.10 Summary for Substrates Selection

Advances are also expected in selecting the most appropriate substrates for deposition. To summarize the previous discussion, the general requirements for successful substrate include the following:

1. Optical quality of transparency to let light reach the photoactive layer.
2. Smoothness in nanometer range to provide a surface that will promote high-quality deposition of subsequent layers and prevent the penetration of potential substrate irregularities into device layers.
3. Ability to support processing at high temperatures.
4. Good dimensional stability.
5. Good resistance to chemicals used during processing.
6. Low water absorption.

Thus, a wide choice of substrates is available and ranges from typical glass, polymers (PET, or polycarbonate) and metals such as stainless steel. Polymers have transparencies that are almost as good as glass and have better elasticity, the fall behind in UV and dimensional stability, as well as processing temperatures. Metals have all the advantages in terms of all physical, mechanical, and chemical properties but they are opaque. Since the efficiency of a solar cell depends on the electrode dimensions and its sheet resistance the sheet resistance of ITO/glass substrate is 10–15  $\Omega$ /square, while the sheet resistance of ITO on PET substrate is around 60  $\Omega$ /square. A rapid decay of the efficiency was shown upon increasing the width of the solar cell.

#### References

- A brief history of OLEDs. [Online]. Available: <https://www.nanowerk.com/spotlight/spotid=57140.php>
- Arbouch I, Karzazi Y, Hammouti B (2014) Organic photovoltaic cells: operating principles, recent developments and current challenges—review. *Phys Chem News* 72:73–84
- Best Research-Cell Efficiency Chart. [Online]. Available: <https://www.nrel.gov/pv/cell-efficiency.html>

- Brinkmann M, Contal C, Kayunkid N, Djuric T, Resel R (2010) Highly oriented and nanotextured films of regioregular poly (3-hexylthiophene) grown by epitaxy on the nanostructured surface of an aromatic substrate. *Macromolecules* 43(18):7604–7610. <https://doi.org/10.1021/ma101313m>
- Fthenakis V (2012) Third generation photovoltaics. [Online]. Available: <https://torl.biblioboard.com/content/1c479981-4815-4497-a712-0bcdbfe9860d?organizationId=1f7368e7-f10b-49a1-8ced-2d9476279974>
- Galagan Y, Andriess R (2012) Organic photovoltaics: technologies and manufacturing. In: *Third generation photovoltaics*, InTech. <https://doi.org/10.5772/25901>
- Inktec
- Murali MG, Rao AD, Yadav S, Ramamurthy PC (2015) Narrow band gap conjugated polymer for improving the photovoltaic performance of P3HT:PCBM ternary blend bulk heterojunction solar cells. *Polym Chem* 6(6):962–972. <https://doi.org/10.1039/C4PY01274G>
- Organic Photovoltaic Solar Cells. [Online]. Available: <https://www.nrel.gov/pv/organic-photovoltaic-solar-cells.html>
- Phenyl-C61-butyric acid methyl ester (2021) Wikipedia. [Online]. Available: [https://en.wikipedia.org/w/index.php?title=Phenyl-C61-butyric\\_acid\\_methyl\\_ester&oldid=1027259346](https://en.wikipedia.org/w/index.php?title=Phenyl-C61-butyric_acid_methyl_ester&oldid=1027259346)
- P3HT Polymer, Reduced to Clear CAS 104934–50–1. Ossila. [Online]. Available: <https://www.ossila.com/products/p3ht>
- Ryu HS, Park SY, Lee TH, Kim JY, Woo HY (2020) Recent progress in indoor organic photovoltaics. *Nanoscale* 12(10):5792–5804. <https://doi.org/10.1039/D0NR00816H>
- Shaban M, Benghanem M, Almohammed A, Rabia M (2021) Optimization of the active layer P3HT: PCBM for organic solar cell. *Coatings* 11(7):863. <https://doi.org/10.3390/coatings11070863>
- Sharma T et al (2022) Recent progress in advanced organic photovoltaics: emerging techniques and materials. *ChemSusChem* 15(5). <https://doi.org/10.1002/cssc.202101067>
- Yu J, Zheng Y, Huang J (2014) Towards high performance organic photovoltaic cells: a review of recent development in organic photovoltaics. *Polymers* 6:2473–2509. <https://doi.org/10.3390/polym6092473>